buildings

MDPI

Article

Mathematical Modelling for Predicting Thermal Properties of Selected Limestone

Abdulla A. Sharo [1,2], Samer R. Rabab'ah [1,*], Mohammad O. Taamneh [1], Hussein Aldeeky [3] and Haneen Al Akhrass [1]

1 Department of Civil Engineering, Jordan University of Science and Technology, Irbid 22110, Jordan
2 Civil Engineering Program, Al Ain University, Abu Dhabi P.O. Box 112612, United Arab Emirates
3 Civil Engineering Department, College of Engineering, The Hashemite University, P.O. Box 150459, Zarqa 13115, Jordan
* Correspondence: srrababah@just.edu.jo

Abstract: Due to a lack of geotechnical and geothermal studies on Jordanian limestone, this paper aims to provide the thermal properties, including thermal conductivity, thermal diffusivity, and specific heat, using the Hot Disk Transient Plane Source (TPS) 2200 method. It also aims to provide a set of mathematical models through which the thermal properties can be indirectly predicted from the rocks' physical and engineering properties. One hundred cylindrical rock specimens with a height of 20 cm and a diameter of 10 cm were extracted and prepared. The results showed that the thermal conductivity values ranged between (1.931–3.468) (W/(m × k)), thermal diffusivity (1.032–1.81) (mm^2/s), and specific heat (1.57–2.563) ((MJ)/(m^3 × K)). The results also suggest a direct relationship between conductivity and diffusivity and an inverse relationship between conductivity and specific heat. On the other hand, the results indicate the direct relationship between the conductivity and diffusivity, and the inverse relationship between the specific heat and density, hardness, sound velocity, and rock strength; the opposite happens when the rock's porosity is considered. Simple regression, multivariate regression, and the backpropagation–artificial neural network (BP–ANN) approach were utilized to predict the thermal properties of limestone. Results indicated that the ANN model provided superior prediction performance compared to other models.

Keywords: conductivity; diffusivity; specific heat; TPS; construction materials

Citation: Sharo, A.A.; Rabab'ah, S.R.; Taamneh, M.O.; Aldeeky, H.; Al Akhrass, H. Mathematical Modelling for Predicting Thermal Properties of Selected Limestone. *Buildings* **2022**, *12*, 2063. https://doi.org/10.3390/buildings12122063

Academic Editor: Kian Jon Chua

Received: 10 October 2022
Accepted: 14 November 2022
Published: 24 November 2022

1. Introduction

The knowledge of the thermal properties of building stones is important for building envelope thermal insulation, especially in very hot, very cold, and undeveloped countries, for energy saving [1]. Rock science's most prominent thermal properties are thermal conductivity, diffusivity, and specific heat [2]. Thermal conductivity is the ability of a material to conduct heat. It is defined as: "the rate of heat transfer through a unit thickness of the material per unit area per unit temperature difference" [3]. Thermal conductivity, denoted by (k), is the ability to transfer heat per unit of time and the unit surface area divided by the temperature difference [4]. Heat capacity is the ratio of heat transferred to an object and its temperature rise. In science and engineering, expressing heat capacity in terms of a unit mass is typically more practical. Therefore, the specific heat denoted by (c) is defined as the heat capacity per unit mass of material [4]. Thermal diffusivity, denoted by (α), is the thermal conductivity divided by density and specific heat; it represents how fast heat diffuses through a material [3]. Mathematically, thermal properties can be defined by the following equations:

$$k = \frac{Q * \Delta L}{A * \Delta T} \quad (1)$$

$$c = \frac{q}{m * \Delta T} \quad (2)$$

$$\alpha = \frac{Heat\ conducted}{Heat\ stored} = \frac{k}{\rho\, C} \quad (3)$$

where k is the thermal conductivity (W/(m × K)), Q is the amount of heat (W), ΔL is the material thickness (m), A is the cross-sectional area (m^2), ΔT is the temperature difference (K), c is the specific heat (J/(kg × K)), q is the change in thermal energy (J), m is the mass of the specimen (kg), α is the thermal diffusivity (m^2/s), and ρ is the density of the material (kg/m^3).

Thermal properties vary according to some physical properties of rocks. The rock's mineral composition is considered one of the most important factors affecting the thermal properties of the rock. Other factors such as porosity, water content, temperature, and pressure [5–7] also influence the thermal properties of rock. Sun et al. [7] investigated the effect of temperature, water content, and porosity on the thermal properties and porosity of sandstone rock in France. The results showed that heating the rock to 400 °C reduced the adhered, combined, and structural water content, lowering thermal conductivity and diffusivity and changing specific heat. Sun et al. [7] concluded that decreasing water content and increasing porosity reduces rock conductivity and diffusivity. This was also concluded by [8] in their study of the rocks on the island of Cyprus, and by [9] in their study on clayey and chalky limestone, as they found that the conductivity and diffusivity are increased in the wet conditions. Labus and Labus [5] discussed the inverse relation between thermal conductivity and temperature and the direct relation between thermal conductivity and pressure. Khandelwal [10] found that water encourages heat movement through the rocks, and external pressure directly affects thermal conductivity by closing and welding fissures that restrict or block heat transfer. In addition to the previous factors, Stylianou et al. [8] concluded that for the same type of rock, the conductivity and diffusivity values increase as the geological age increases. The reason for this increase, as Jones [11] pointed out, is that metamorphism and alteration operations on rock mineralogical composition increase thermal conductivity and diffusivity. Finally, rock structure greatly affects thermal conductivity: crystalline rock has a higher thermal conductivity than amorphous or vitreous rock, and thermal conductivity increases with crystallization [12].

Recently, hot disk transient technique has gained prominence as a tool for measuring thermal properties quickly and accurately [13]. Measuring thermal properties of rocks can be implemented under small-scale conditions by laboratory tests or in situ under large-scale conditions by applying the transient techniques [14] where known thermal energy generated from a known thermal energy source is employed. After that, the temperature change with time is monitored and recorded [15].

Several attempts were made to estimate rock's thermal properties from several rock indices indirectly. Boulanouar et al. [16] concluded that the thermal conductivity of sedimentary, metamorphic, and magmatic rocks could be estimated indirectly from ultrasonic pulse velocity through a strong linear model with $R^2 = 0.85$. Additionally, thermal conductivity was linked with dry density, porosity, ultrasonic pulse velocity, and uniaxial compressive strength through a set of strong models by Yaşar et al. [1] in limestone, dolomite, marble, travertine, sandstone, siltstone, and basalt, and by Özkahraman et al. [17] in limestone and travertine. In clayey and chalky limestone, Çanakci et al. [9] concluded that the thermal conductivity could be estimated through strong models which link thermal conductivity with dry density, porosity, and water absorption.

Researchers have recently adopted the ANN to predict and estimate engineering properties to solve more complex and real-life problems. ANN is a non-parametric model with the great ability to learn complicated non-linear connections between variables implicitly. The ANN learning algorithm with backpropagation (B.P.) is a well-established approach for handling various classification and forecasting issues [18]. Researchers utilized ANN to deal with various difficulties for numerous Civil and Geotechnical Engineering applications. Maji and Sitharam [19] proposed two artificial neural network (ANN) models (using feed-forward backpropagation (FFBP) and radial basis function (RBF)) to predict the elastic modulus of jointed rocks using data from uniaxial and triaxial compression experiments, taking into account different joint arrangements and confining pressures. Bui et al. [20] predicted building energy consumption using the electromagnetism-based firefly algorithm–artificial neural network (EFA–ANN). Two datasets calculate heating and cooling loads. Façade energy consumption and building dimensions were collected from each dataset. Comparisons with other methods verified model performance. The results showed that EFA–ANN helped civil engineers and construction managers design energy-efficient structures. Singh et al. [21] used the ANN and adaptive neuro-fuzzy inference system (ANFIS) to investigate the thermal conductivity and other fundamental properties of rocks. Six different ANN and ANFIS models are compared to assess their capabilities. P-wave velocity, porosity, bulk density, and the rock's uniaxial compressive strength were the input parameters that were used to predict thermal conductivity.

Limestone is used in many engineering applications; the most important is its use as a construction material in buildings' facades and columns (Figure 1). It possesses many desired properties, such as hardness, thermal insulation, aesthetic view, and indoor humidity prevention. Unfortunately, few studies have evaluated the physical engineering properties of lime building stone [22], especially studies related to heat flow and thermal properties of sedimentary rock [5].

Figure 1. Application of limestone in building's facades and columns.

This research paper aims to provide the thermal properties of lime building stone through the TPS 2200 method and explain how these properties are affected by the physical and engineering properties of the rocks. Despite the advantages of the Hot Disk Transient Plane Source (TPS) 2200 method, it is expensive. For this reason, the second goal of this research is to create a set of statistical models that enable the site engineer to indirectly predict the thermal properties of the rock from easy, simple, inexpensive, and non-destructive tests. To achieve the second goal, regression analysis, a well-known statistical analytical technique, and artificial neural networks (ANN) were implemented on a set of data that included the thermal, physical, and engineering properties of lime building stone to develop a set of statistical models to predict thermal properties from the physical (such as hardness, density, the velocity of sound waves, and porosity) and engineering (such as uniaxial compressive strength and point load strength) properties of the rock.

2. Materials and Methods

2.1. Rock Specimens Preparation

Limestone is found in huge quantities and at various depths in Jordan. This rock underlies 90% of Jordan's land area. According to the Natural Resources Authority [23], which is in charge of locating Jordan's raw minerals and natural resources, limestone stone is primarily sourced from Ajloun, the north-western part of Jordan (source 1), and Ruweished, the eastern part of Jordan (source 2). Due to its shallow depth in Ruweished, where it becomes superficial after removing the half-meter-thick earthen layer, and because it is exposed at the soil surface in Ajloun, lime building stone is extracted from these two sites. In contrast, the existence of limestone at great depths in southern Jordan led to a major decline in its exploitation activity [23]. To obtain a representative specimen, several stone blocks were obtained from both areas, as shown in Figure 2. A total of 100 block specimens (50 specimens from each location) were collected to perform this study with a minimum size of approximately 50 cm. Cylindrical rock cores with a diameter of 10.0 cm and a length-to-diameter ratio of 2:1 were prepared from each block, according to ASTM D4543 standard [24], as shown in Figure 3.

Figure 2. Stone blocks from both studied areas.

Figure 3. After preparation and marking, one hundred cylindrical core specimens (Height = 20 cm, Diameter = 10 cm).

2.2. Method and Laboratory Tests

After preparing the cylindrical rock core specimens, each specimen was dried in an oven at 105 °C for 24 h to extract the water absorbed by the rock specimens during the collection and preparation stage, which included polishing, coring, and diamond bit sawing. After that, a series of tests were conducted to achieve the objectives of this study. The tests conducted in this study were divided into two parts, the first is the tests related to the thermal properties of rock specimens, and the second is the tests related to rock specimens' physical and engineering properties. All the tests were performed on oven-dried specimens at room temperature and pressure.

2.2.1. Thermal Properties Determination

The TPS method was used in this investigation to determine the thermal characteristics of the limestone rock specimens. The hot disk transient technique is a non-destructive, high-accuracy method with easy-to-prepare specimens [13,25]. The main advantages of the hot disk technique include a wide range of measurable thermal conductivity, from 0.005 (W/(m × k)) to 500 (W/(m × k)), over a wide temperature range from −50 °C to 750 °C. The experiment setup is schematically shown in Figure 4.

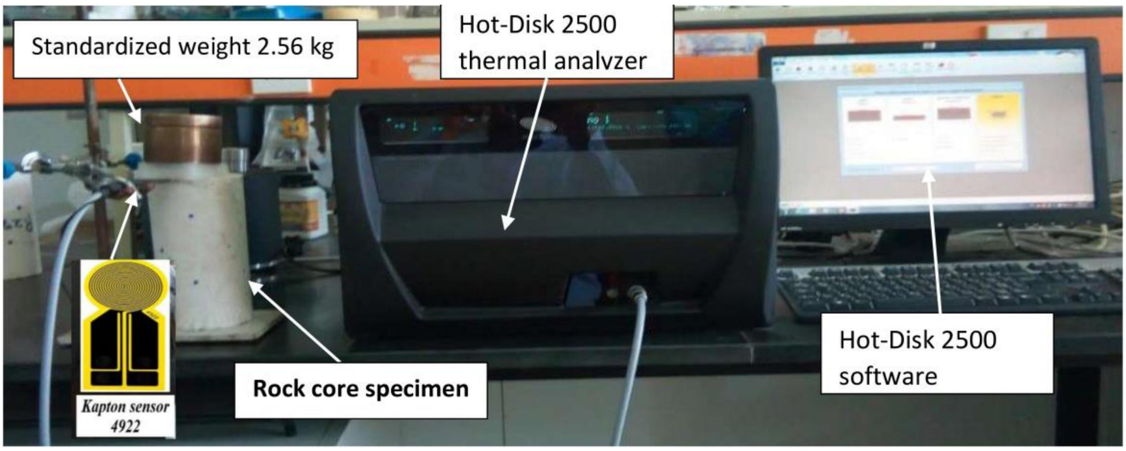

Figure 4. The schematic of the single-sided experimental specimen setup was used in this study.

Nickel (Ni) is used for the TPS sensor because of its high thermal resistivity. The double-spiral-shaped sensor has four electrical connections: two for heat current and one for detecting. The sensor works as a heat source to raise the specimen temperature and a thermometer to measure the change. The thermal conductivity can be computed from the reported temperature rise [26]. The sensor is believed to be in infinity. Therefore, the measurement period must be managed so that thermal penetration depth does not exceed specimen thickness. There are several types of sensors that may be used in this method, the Kapton sensor (4922) is used in this study with 29.2 (mm) in diameter, 1000 (mW) injected power, 160 (s) measurement time, and (18–21) (mm) penetration depth [27].

The TPS sensor was positioned on a rock surface (a smooth surface without outcrops or cracks). The sensor was then insulated to avoid heat leakage. Figure 4 shows that the sensor was loaded with 2.56 kg to guarantee proper sensor-to-sample contact. After that, the Hot Desk Thermal Constant Analyzer software calculated the numerical results, which included thermal conductivity, thermal diffusivity, and specific heat.

2.2.2. Physical and Engineering Properties Determination

After drying the specimens in an oven at 105 °C for 24 h, dry density (ρd) was measured in (g/cm^3) for each specimen by the ratio between dry weight and volume [28]. The Ultrasonic Pulse Velocity (V_p) test was carried out according to the recommendations of ASTM D2845 [29] by using PUNDIT Pulse (Portable Ultrasonic Non-Destructive Digital Indicating Tester) (MATEST (S.r.l)/TREVIOLO 24048; ITALY) with two transducers having a frequency of 54 kHz and 6.4 mm wavelength. Five velocities for each specimen were calculated, and their averaging was taken. Schmidt Hammer Rebound (H_r) test was performed on each core specimen according to the recommendations in [30] as a rock hardness index. Apparent specific gravity (Gs) and porosity (n) values for each specimen were determined according to procedures suggested by [28], where the oven-dried specimens were soaked in a water-filled tank. The weight of the specimen was monitored for 22 days until it began to demonstrate a constant weight to ensure that all specimens were fully saturated. In more detail, the weights of all samples began to stabilize after 17 days of soaking, and they were monitored for another five days to ensure that the constant weight had been achieved. Uniaxial Compressive Strength (UCS) was carried out on oven-dried specimens according to the ASTM D7012 [31] recommendations at a constant strain rate on the specimens with length-to-diameter equal to 2. Point load strength ($Is_{(50)}$) on irregular rock fragments was also carried out according to ASTM D5731 [32].

3. Results and Discussion

3.1. Thermal Properties of Limestone Rock

The statistical parameters for thermal conductivity (k), thermal diffusivity (α), and specific heat (c) for both rocks are shown in Tables 1 and 2.

Table 1. Statistical parameters for the thermal properties.

Property	Min.	Max.	Avg.	Standard Deviation	Coefficient of Variation
k (W/(m*k))	1.931	3.468	2.861	0.327	11.45
α (mm^2/s)	1.032	1.810	1.323	0.123	9.31
c ((MJ)/(m^3*K))	1.570	2.563	2.157	0.192	8.91

Table 2. Statistical parameters for physical and engineering properties.

Property	Unit	No. of Specimens	Min.	Max.	Avg.	Standard Deviation	Coefficient of Variation
ρ_d	g/cm^3	100	2.521	2.692	2.521	0.113	4.492
Gs	-	100	2.677	2.714	2.677	0.031	1.16
Hr	-	100	34.423	43.65	34.422	4.912	14.269
UCS	MPa	100	81.341	138.39	81.341	20.448	25.139
$Is_{(50)}$	MPa	100	3.357	4.825	3.357	0.579	17.241
n%	-	100	5.845	15.924	5.846	3.265	55.87
V_p	m/s	100	5476.3	6366.3	5476.32	618.228	11.289

An independent specimens *t*-test analysis was used to determine whether there is a statistically significant difference between the means of both rocks' thermal, physical, and engineering properties. The results of the *t*-test indicate a statistically significant difference in some thermal, physical, and engineering properties between both sources, especially in porosity, and specific heat, where the calculated *p*-value for each property is close to zero (i.e., less than 0.05) and the higher porosity of the limestone (source 2) specimens had an important impact on obtaining lower thermal properties.

From the data found for rocks, it can be concluded that the thermal conductivity increases with increasing thermal diffusivity and decreases with increasing heat capacity (Figure 5). This can be explained by the fact that the material with high thermal conductivity will have a large thermal diffusivity and a low heat capacity. The larger the thermal diffusivity, the faster the heat transmission through the medium, which is consistent with thermal conductivity. On the other hand, a small thermal conductivity value (i.e., a small value of thermal diffusivity) means that the material mostly absorbs heat, and a small amount of the heat will be transmitted through the medium [3,33]. Additionally, increasing thermal conductivity means that further heat will be extracted from the source, which also means the diffusivity of absorbed heat becomes quicker [5].

Cermak and Rybach [34] reported that the range of thermal conductivity for rock is (0.4–7) (W/)m × k)), and Çanakci et al. [9] also reported that the range of thermal conductivity for building stones is (1.163–8.6) (W/)m × k)). Thermal conductivity values found in this study are within these two ranges. Additionally, the thermal conductivity values found in this study occupy lower ranges than those specified by [9,34]. This can be attributed to the presence of quartz in very low percentages (less than 1%) in both types of rocks extracted from both regions, which is considered a good thermal conductor, where the range of thermal conductivity for quartz is (6.5–11.3) (W/)m × k)) [5]. Pechnig et al. [35] concluded that the thermal conductivity increased with quartz/feldspar ratios. The thermal conductivity of Kristallsandstein rock (90% quartz and 6% feldspar) is higher than the thermal conductivity of Schilfsandstein rock (57% quartz and 35% feldspar).

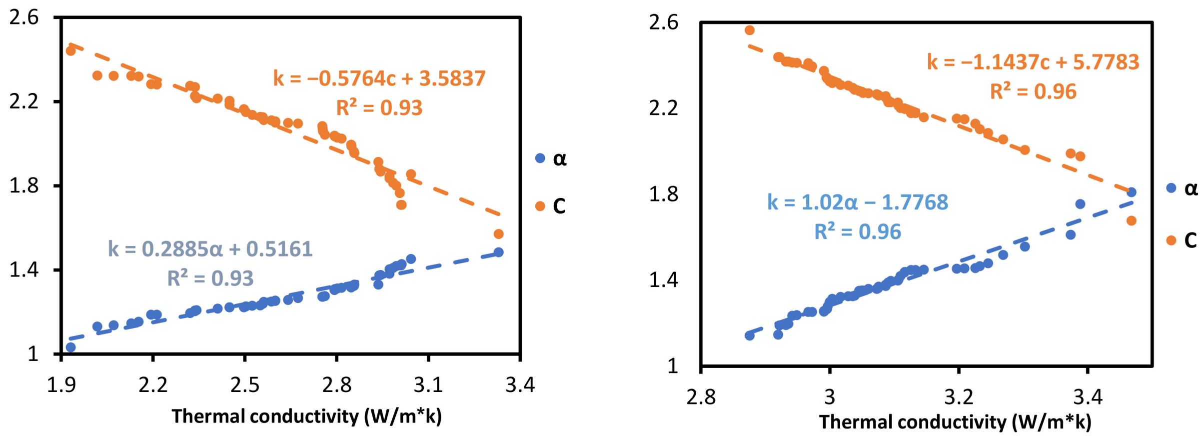

(**a**) (**b**)

Figure 5. Thermal conductivity versus thermal diffusivity and specific heat for limestone rocks in (**a**) source 1 and (**b**) source 2 ((k) in a unit of (W/(m × K)), (α) in a unit of (mm^2/s), and (C) in a unit of (MJ)/(m^3 × K)).

3.2. Regression Analysis for Predicting Thermal Properties

In this study, thermal properties of rock, which require costly technology to estimate, were considered as dependent variables, and the physical properties, including ρ_d, H_r, V_p, and n%, which can be found directly by easy, simple, inexpensive, and non-destructive tests, were considered as independent variables. Additionally, to present a more comprehensive study, engineering properties, including UCS and Is(50), were entered into the list of the independent variables.

Statistical analysis methods, including hypothesis testing, analysis of variance (ANOVA), and regression analysis, require that the dependent variable is normally distributed. In this study, the Kolmogorov–Smirnov test was used by the SPSS program to check whether the dependent variables are normally distributed with a significant level (0.05). Table 3 shows the normality test results, where the calculated *p*-value for dependent variables in both rocks is more than (0.05), which means accepting the Null hypothesis and rejecting the alternative hypothesis. Therefore, the dependent variables are normally distributed, and parametric statistical tests can be used.

Table 3. Results of Kolmogorov–Smirnov test for normality checking *.

	Source 1			Source 2		
DV	**Statistic**	**Df ***	**Sig.**	**Statistic**	**Df ***	**Sig.**
k	0.082	50	0.200	0.097	50	0.200
α	0.118	50	0.082	0.111	50	0.172
c	0.102	50	0.200	0.093	50	0.200

* Df: degree of freedom, sig. Significant level (0.05).

3.3. Simple Regression Analysis

In simple regression analysis, only one independent variable can predict the dependent variable. Four curve-fitting relationships were used: exponential, power, logarithmic, and linear. The mathematical formula for each model is shown in Table 4, where y_p is the predicted value, x is the input parameter, c is the regression constant, and b is the regression coefficient.

Table 4. Mathematical equations were obtained from this study.

Independent Variable	Unit	Equation (Source 1)	R^2	VAF%	RMSE	Equation (Source 2)	R^2	VAF%	RMSE
ρ d	g/cm^3	$k = 3.3716\ \rho_d - 5.7177$ $c = 207.92\ \rho_d^{-4.719}$ $\alpha = 3.4696\ \rho_d - 7.6889$	0.66 0.64 0.64	66 62 64	0.07 0.09 0.07	$k = 3.1391\ \rho_d - 4.9995$ $c = -1.9003\ \rho_d + 6.6864$ $\alpha = 0.9539\ \rho_d - 1.0435$	0.89 0.90 0.92	89 90 92	0.11 0.05 0.02
Gs	-	$k = 9.0146\ (Gs) - 21.314$ $c = -10.26(Gs) + 30.02$ $\alpha = 8.8217(Gs) - 22.507$	0.1 0.1 0.09	3.56 14.66 5	1.3 1.8 1.7	$k = 14.286\ (\mathbf{Gs}) - 35.191$ $c = -9.9973(\mathbf{Gs}) + 28.536$ $\boldsymbol{\alpha} = 4.819\ (Gs) - 11.483$	0.38 0.51 0.48	4.51 14.53 3.67	19.94 0.87 0.81
Vp	m/s	$k = 1.1302e^{0.0002\ Vp}$ $c = -0.0006\ Vp + 5.791$ $\alpha = 0.149e^{0.0004\ Vp}$	0.71 0.66 0.65	60 66 63	0.64 0.09 0.26	$k = 2.7834\ln(Vp) - 21.055$ $c = -0.0003\ Vp + 3.7657$ $\alpha = 0.0002\ Vp + 0.4315$	0.82 0.87 0.87	82 86 85	0.13 0.21 0.15
Hr	-	$k = 0.066\ Hr + 0.518$ $c = -0.0749\ Hr + 5.151$ $\alpha = 0.0672\ Hr - 1.2321$	0.88 0.82 0.83	88 82 83	0.04 0.06 0.05	$k = 3.2977\ln(Hr) - 8.577$ $c = -0.0659\ Hr + 4.0479$ $\alpha = 0.033\ Hr + 0.2842$	0.96 0.95 0.96	96 95 96	0.06 0.04 0.02
n%	-	$k = -0.362\ln(n) + 3.5343$ $c = 0.4067\ln(n) + 1.7455$ $\alpha = -0.361\ln(n) + 1.8182$	0.63 0.58 0.58	63 58 58	0.07 0.09 0.08	$k = -0.0925\ n + 3.3856$ $c = 0.3897\ln(n) + 1.2849$ $\alpha = -0.0278\ n + 1.5022$	0.90 0.90 0.90	90 90 91	0.10 0.06 0.02
UCS	MPa	$k = 0.0075\ UCS + 2.3565$ $c = -0.0085\ UCS + 3.0691$ $\alpha = 0.0075\ UCS + 0.6455$	0.87 0.80 0.79	87 80 79	0.04 0.06 0.06	$k = 1.7287\ln(UCS) - 4.5797$ $c = -0.0159\ UCS + 3.1098$ $\alpha = 0.0079\ UCS + 0.7577$	0.87 0.84 0.83	88 84 83	0.11 0.07 0.04
$Is_{(50)}$	MPa	$k = 0.371\ Is_{(50)} + 1.6507$ $c = -0.4326\ Is_{(50)} + 3.9225$ $\alpha = 0.3852\ Is_{(50)} - 0.1196$	0.82 0.82 0.81	82 82 81	0.05 0.06 0.05	$k = 0.6825\ e^{0.4718\ Is(50)}$ $c = -0.6648\ Is_{(50)} + 3.96$ $\alpha = 0.6056\ Is_{(50)}^{\ 0.7124}$	0.85 0.72 0.72	85 72 71	0.12 0.09 0.05

Based on several statistical indices, such as coefficient of determination (R^2), Root Mean Square Error (*RMSE*), and Variance Accounted For, four predicted models were evaluated, and the strongest one was chosen (*VAF*). R^2 is a relative measure of the proportion of the dependent variable's variance that the model explains (R^2 can range from 0 to 1); *RMSE* is an absolute measure of the average distance that data points fall from the regression line (*RMSE* is in the units of the dependent variable). VAF is frequently employed to validate the accuracy of a model by comparing the actual output to the estimated output (*VAF* can range from 0% to 100%). Therefore, a regression model was considered the strongest one if (R^2) was close to 1, (*VAF*) was close to 100%, and (*RMSE*) was close to zero [36–38]. Equation of each statistical parameter is shown below:

$$R^2 = 1 - \left(\frac{\sum_{i=1}^{n} \left(y_m - y_p \right)^2}{\sum_{i=1}^{n} \left(y_m - y_a \right)^2} \right) \tag{4}$$

$$RMSE = \sqrt{\frac{1}{n} \sum_{i=1}^{n} \left(y_m - y_p \right)^2} \tag{5}$$

$$VAF = \left\{ 1 - \left(\frac{VAR\left(y_m - y_p \right)}{VAR(ym)} \right) \right\} \times 100\ \% \tag{6}$$

where y_m is the measured value, y_p is the predicted value, y_a is the average of the measured value, and n is the total number of data.

Conductivity, diffusivity, and specific heat are linked with physical properties, including ρ_d, Gs, V_p, H_r, and n%, with strong relationships, and the graph for each model is shown in Figures 6, 7, 8, 9, 10, respectively. There is a direct relationship between conductivity and diffusivity (i.e., an inverse relationship of the specific heat) with density, hardness, and pulse velocity. An inverse relationship between the conductivity and diffusivity (i.e., a direct relationship of the specific heat) was observed when the thermal properties were linked with the rock's porosity.

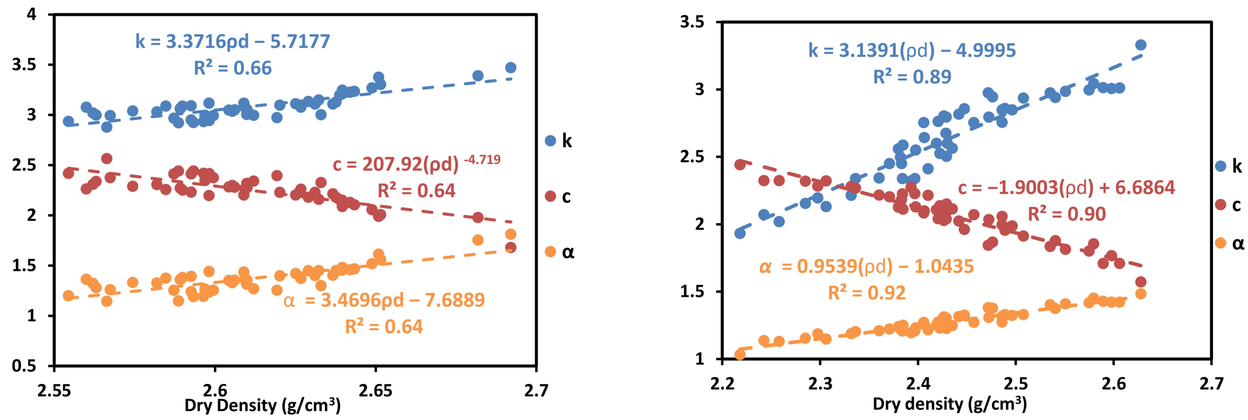

(**a**) (**b**)

Figure 6. Thermal properties vs. dry density in (**a**) source 1 and (**b**) source 2((k) in a unit of (W/(m × K)), (α) in a unit of (mm^2/s), and (c) in a unit of (MJ)/(m^3 × K)).

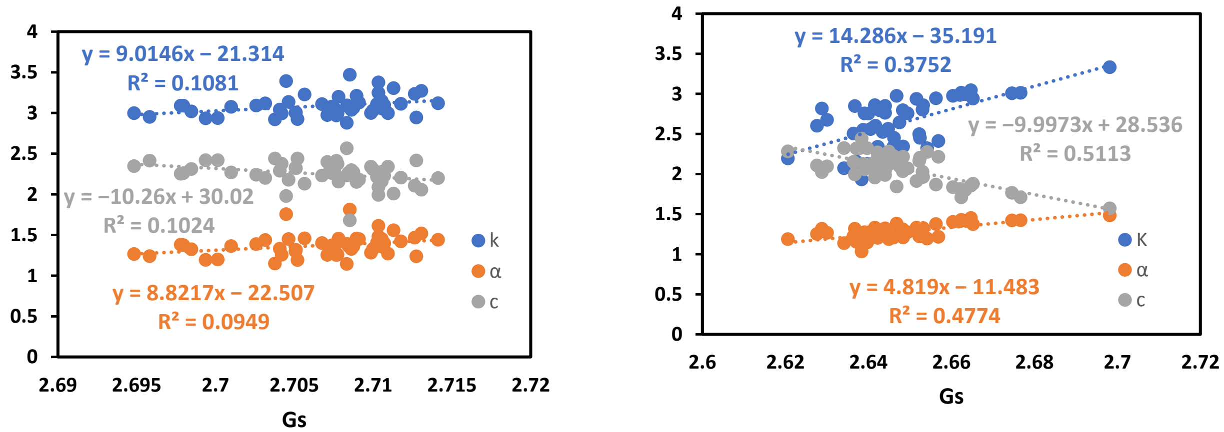

(**a**) (**b**)

Figure 7. Thermal properties vs. Specific gravity in (**a**) source 1 and (**b**) source 2 ((k) in a unit of (W/(m × K)), (α) in a unit of (mm^2/s), and (c) in a unit of (MJ)/(m^3 × K)).

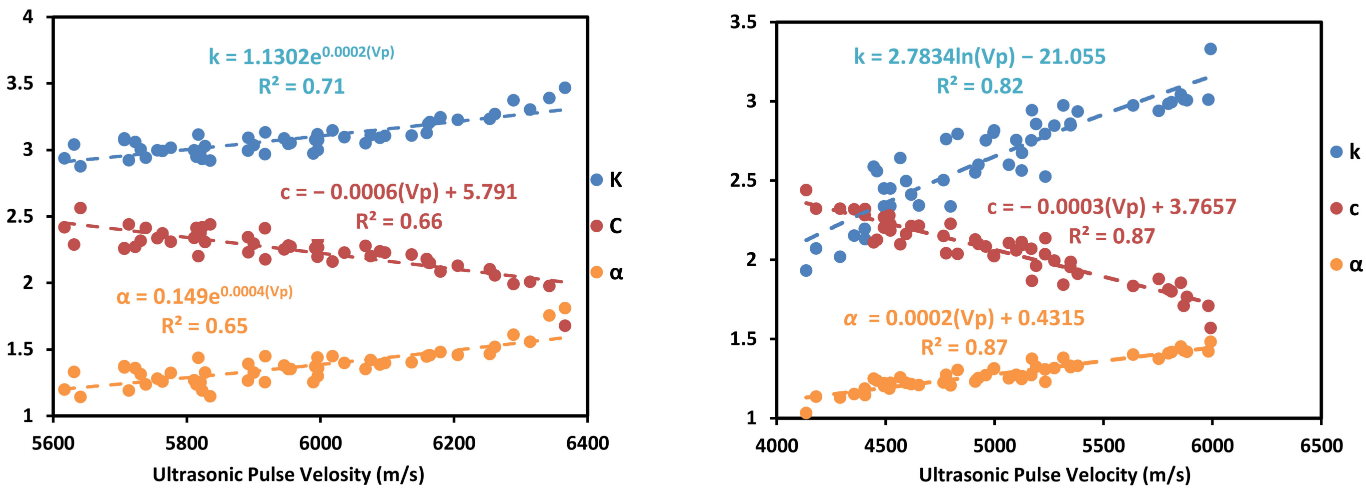

(**a**) (**b**)

Figure 8. Thermal properties vs. pulse velocity in (**a**) source 1 and (**b**) source 2 ((k) in a unit of (W/(m × K)), (α) in a unit of (mm^2/s), and (c) in a unit of (MJ)/(m^3 × K)).

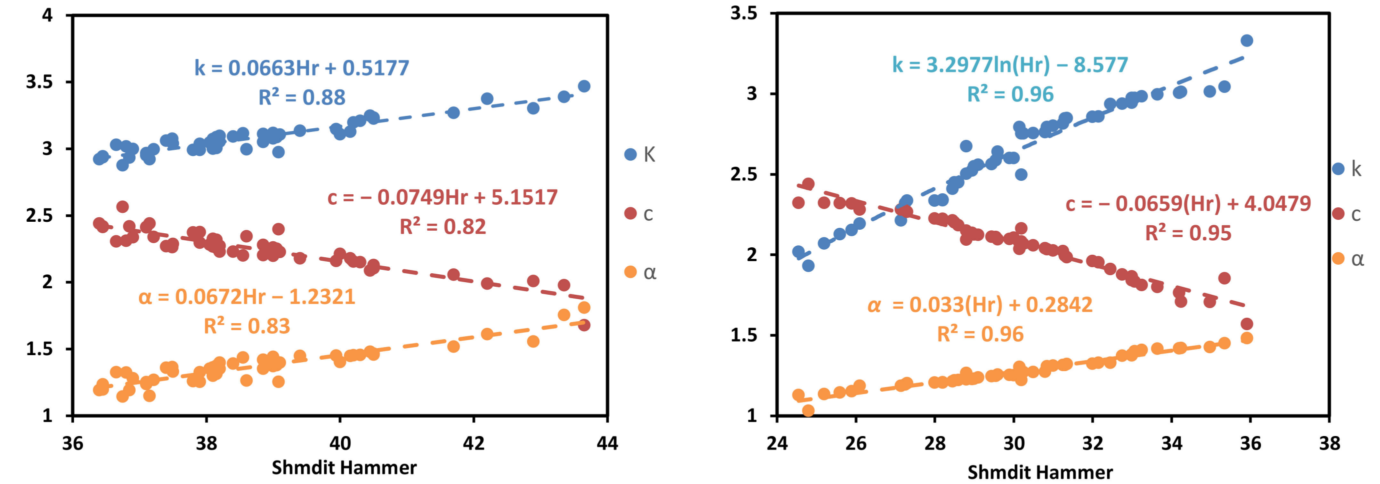

(**a**) (**b**)

Figure 9. Thermal properties vs. hardness in (**a**) source 1 and (**b**) source 2 ((k) in a unit of (W/(m*K)), (α) in a unit of (mm^2/s), and (c) in a unit of (MJ)/(m^3 *K)).

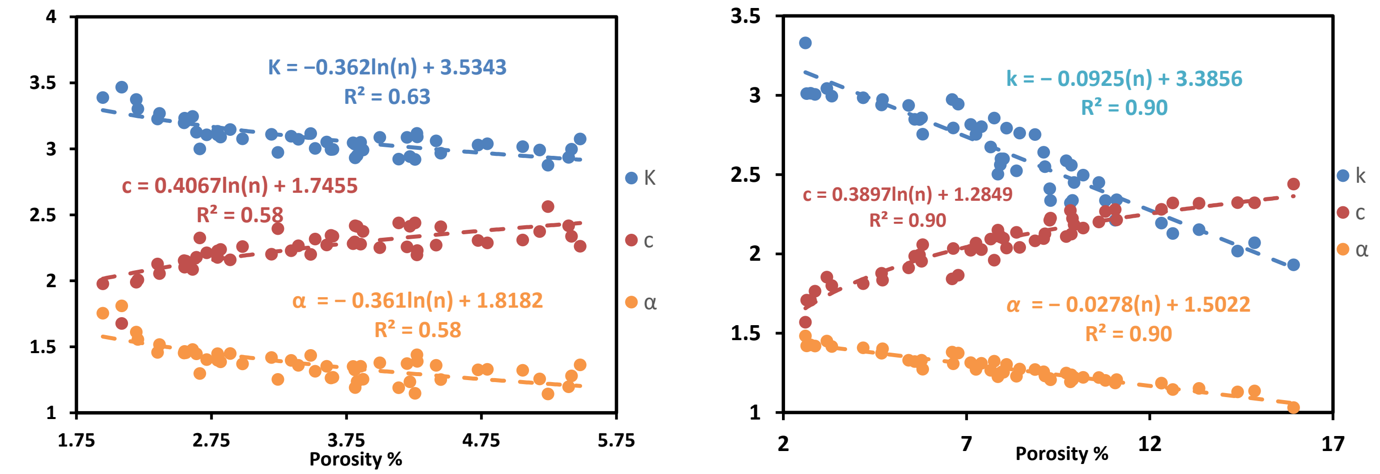

(**a**) (**b**)

Figure 10. Thermal properties vs. Porosity in (**a**) source 1 and (**b**) source 2 ((k) in a unit of (W/(m × K)), (α) in a unit of (mm^2/s), and (c) in a unit of ((MJ)/(m^3 × K)).

The presented results through Figures 6–10 regarding the relationship between thermal properties and ρd, Gs, Vp, Hr, and n % are consistent with the findings of many researchers. Boulanouar et al. [16], Yaşar et al. [1], Özkahraman et al. [17], and Çanakci et al. [9] pointed out the direct relationship of thermal conductivity with ρd, Vp, and Hr. Additionally, Pechnig et al. [35] indicated that rocks' thermal conductivity decreased with porosity.

Additionally, the relationship between thermal conductivity and porosity has been compared between the results of this study and with what some researchers have found, including Özkahraman et al. [17] on limestone and travertine and Çanakci et al. [9] on clayey and chalky limestone, Pichugin et al. [39] on different types of sedimentary rocks, and Zeb et al. [40] on porous limestone as shown in Figure 11. In general, it is clear from Figure 11 that there is an inverse relationship between the thermal conductivity and the porosity, but perhaps the reason for the incompatibility between the types of curves is that the relationships are more general and applied to more than one type of rock.

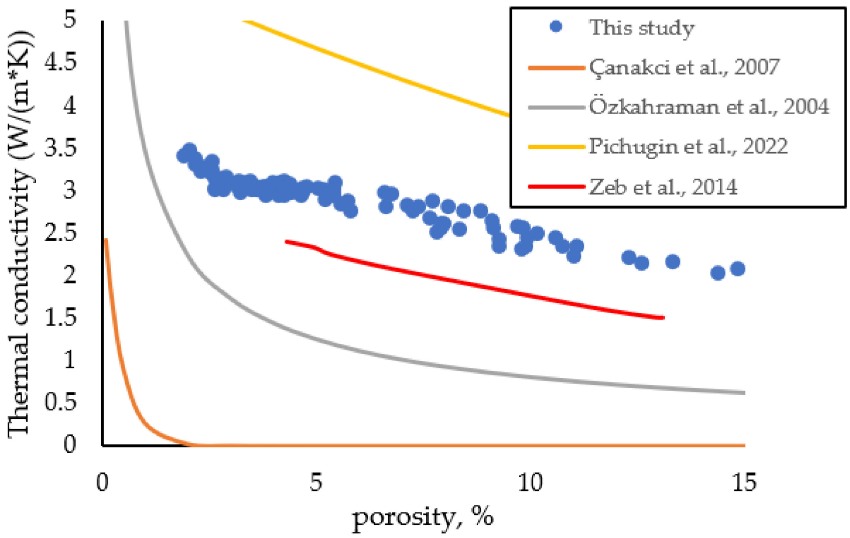

Figure 11. Comparing the relationship between thermal conductivity and porosity based on the results of this study with some previous studies [9,17,35,40].

In the literature, the obtained mathematical models which linked the thermal properties with rock's indices were not specialized to one type of rock, such as limestone, for example, they were more generally for several types of rocks. Chekhonin et al. [41] reported that the trends significantly changed from one type of rock to another, so empirical equations must be unique and not generalized. Hence, the need to create a set of mathematical models specialized in finding the thermal properties of the physical and engineering properties of limestone in Jordan.

In terms of stresses, conductivity, diffusivity, and specific heat are linked with strong relationships with uniaxial compressive strength (Figure 12) and point load strength index (Figure 13). There is a direct relationship between the conductivity and diffusivity (i.e., an inverse relationship of the specific heat) with uniaxial compressive strength and point load strength index.

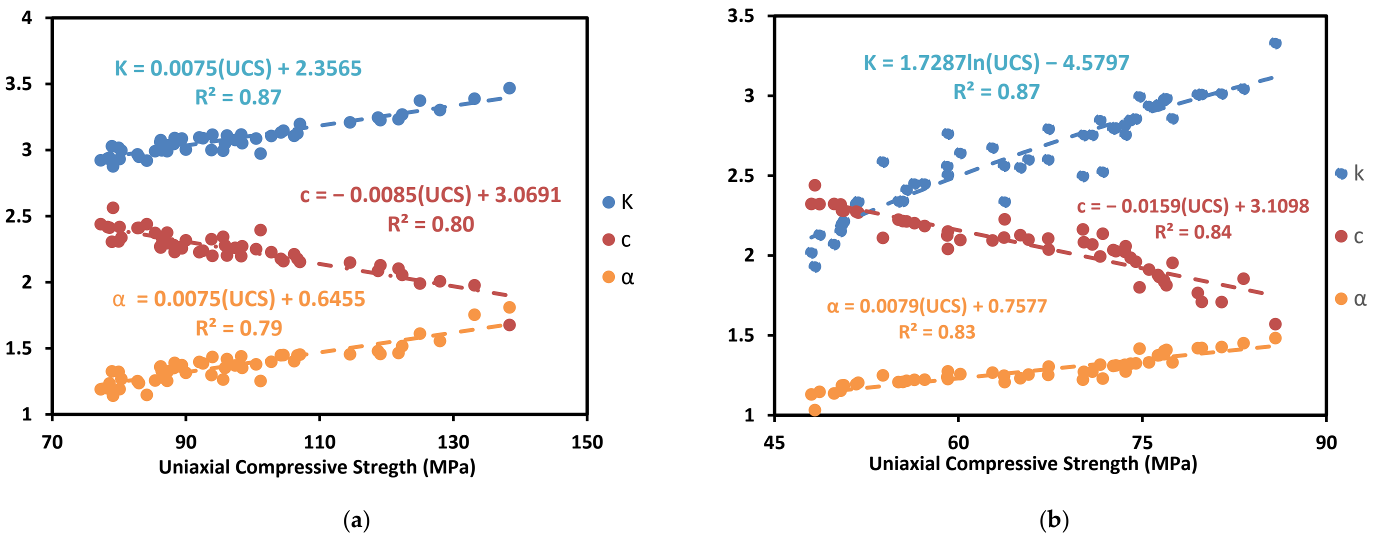

Figure 12. Thermal properties vs. compressive strength in (**a**) source 1 and (**b**) source 2 ((k) in a unit of (W/(m × K)), (α) in a unit of (mm^2/s), and (c) in a unit of (MJ)/(m^3 × K)).

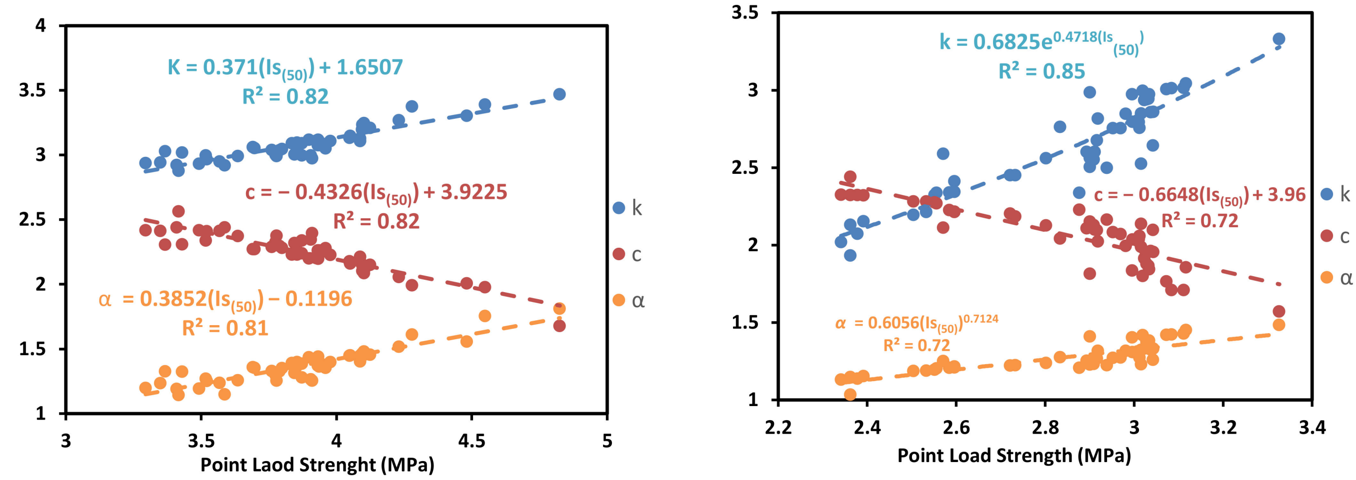

(**a**) (**b**)

Figure 13. Thermal properties vs. point load strength in (**a**) source 1 and (**b**) source 2 ((k) in a unit of (W/(m × K)), (α) in a unit of (mm^2/s), and (c) in a unit of (MJ)/(m^3 × K)).

What can be noted is that the models are stronger for thermal conductivity prediction followed by thermal diffusivity, and are the weakest to the point that they almost do not describe the variance in the specific heat data. This is due to the huge difference in the specific heat properties between the two included rocks, making it very hard to predict this parameter for both. Additionally, the nature of limestone source 1 contains some bedding planes, as shown in Figure 14, which are located at different locations on the specimen; these bedding planes lead to the data being distributed more randomly in source 1.

(**a**) (**b**)

Figure 14. Some of the broken specimens for both included limestone ((**a**) source 1, and (**b**) source 2).

3.4. Multivariate Regression Analysis

Multivariate regression analysis can be used to achieve stronger models for predicting the thermal properties of rocks, which means higher R^2 and VAF and lowest RMSE [42]. Additionally, the rock's thermal properties are a function of rocks' physical, textural, and mineralogical composition (i.e., they do not depend only on a particular rock index). Finally, to learn more about the relationships between the thermal properties and other indices of rock, a multivariate regression analysis was applied in this study as the second stage of regression analysis by considering more than one input parameter.

Multivariate regression analysis requires a linear relationship between dependent and independent variables with a correlation coefficient larger than 0.3 [43]. Additionally, multicollinearity is a known problem in multivariate regression, where two or more independent variables correlate highly. Multicollinearity leads to a non-ideal model. The evaluation of the possibility of the existence of multicollinearity was based on the variation influence factor (VIF). A (VIF) value must be less than 3, 5, or 10 to verify the absence of multicollinearity [44]. By using SPSS, the aforementioned conditions were checked. The correlation coefficient values for linear relationships between the dependent and each category of independent variables are larger than 0.3. Additionally, (VIF) values were checked for each model, and (VIF) values were smaller than 10. Therefore, the multivariate regression analysis can be applied. SPSS program was used to build a multivariate regression model by stepwise method, which excludes the predictors added to the model without making it stronger. Table 5 shows the results of the multivariate regression. From Table 5, the strong correlation between thermal properties and the rock's compressive strength is observed, where the rock's UCS was termed in all models; therefore, the UCS parameter can be considered the most important factor affecting the thermal properties of the rock.

Table 5. Results of multivariate regression models.

Model	R^2	VAF%	RMSE
$k = 2.932 - 0.073(n\%) + 0.004\ (UCS)$	0.94	88	0.04
$\alpha = 6.161 + 0.005\ (UCS) - 4.56(G_s)+2.620(\rho_d) + 0.056\ (n\%)$	0.80	84	0.05
$c = -13.682+7.60(G_s)+1.932(\rho_d) - 0.011(UCS) + 0.386\ (Is_{(50)})$	0.69	84	0.06

3.5. Artificial Neural Network Analysis

In this study, the multilayer perceptron, a kind of ANN, was implemented using the Waikato Environment for Knowledge Analysis (WEKA) software. MLP is a feed-forward network that uses a supervised learning algorithm without any brief assumption about the distribution and pattern in the data. It consists of at least three layers: input, hidden, and output. Each layer consists of several neurons or nodes fully connected to the next layer by weights (Gardner and Dorling, 1998). A weighted sum of the normalized parameter is the input to each node in the hidden layer that modified this sum by a certain activation function and transferred it to the output layer. That output layer signal is a function of the weighted sum signals from the previously hidden layer signals that can be calculated using the following equation.

$$Y' = \sum_{i=1}^{n} (\omega_i * sig(\alpha)_i) + \vartheta \tag{7}$$

Y': The predicted normalized value.
n: Node's number in the hidden layer.
ω_i: Node weight.
$(\alpha)_i$: Sigmoid value for the weighted sum of the inputs to the hidden layer.
ϑ: The output bias.

MLP learns through the training data and assigns the weight for each connection in the model. The predicted value is calculated using the previous equation, and the weight is then adjusted based on the error term between the actual and predicted value and using one of the backpropagation training algorithms to find the weights with the minimum error term [45]. In this study, the sigmoid activation function was used in the hidden layers to handle the nonlinearity in the data and its easy computations [46] compared with the linear activation function for the output layer.

The data were split into two subsets, training and validation, to test the model's performance based on unseen data. The number of nodes was determined using the process suggested by (Shahin et al., 2002). The process is based on starting with a small number of hidden layers and increasing it until no further improvement in the model is represented by the mean absolute error (MAE)) term and correlation coefficient. In addition, a stopping criterion was used to control the training time (epoch number) and avoid the overfitting problem. The number of epochs stops increasing when an adjacent increase in the error term within the training set occurs. Therefore, the final model and the final weights are the ones before the last increase in the error term. A review of the final results of all three models of predicting the rock's thermal properties was included in Table 6 for both training and validation sets. Two hidden layers were used to predict the specific heat values and handle the variation in the data instead of only one hidden layer for the thermal conductivity and diffusivity. Figure 15 represents the goodness of fit between the actual and predicted values of the thermal properties.

Table 6. Results of the multi-layer perceptron (MLP) using WEKA software.

DV	Structure	Training Results			Validation Results		
		R^2	MAE	RMSE	R^2	MAE	RMSE
k	2-2-1	96.07	0.050	0.065	98.03	0.032	0.041
α	7-4-1	86.7	0.036	0.048	75.70	0.023	0.039
c	7-4-2-1	92.16	0.043	0.043	92.08	0.049	0.056

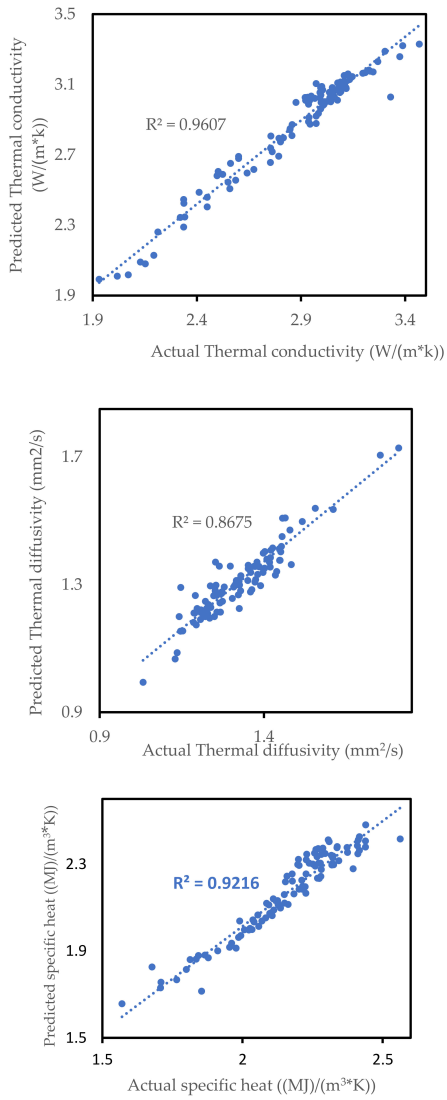

Figure 15. The goodness of fit between the actual and predicted values.

4. Conclusions

The thermal properties covered in this study are thermal conductivity, thermal diffusivity, and specific heat, which are considered the most superior thermal properties in rock science and measured by using the Hot Disk Transient Plane Source (TPS) 2200 as a method for rapid and accurate thermal properties measurement. Based on the results of this study, the following points can be concluded:

1. There is a difference in the thermal properties of the included limestone, especially in the specific heat. This is due to the difference in physical and engineering properties, the variance in the abundance of minerals in it, and the variance in porosity.
2. The results of an independent samples *t*-test analysis indicate a statistically significant difference in the thermal, physical, and engineering properties between rocks, where the calculated *p*-value for each property is close to zero (i.e., less than 0.05).
3. The thermal conductivity increases with the increasing thermal diffusivity and decreases with the increasing heat capacity. Increasing conductivity means that further heat will be extracted from the source, which means the diffusivity of absorbed heat become faster. On the other hand, a small conductivity value means that the material mostly absorbs heat, and a small amount of the heat will be transmitted through the medium.
4. The low thermal conductivity values for studied rocks compared to some other building stones mean that it can be considered as the best and perfect thermal conductor.
5. There is a direct relationship between the conductivity and diffusivity (i.e., an inverse relationship to the specific heat) and the density, hardness, pulse velocity, and rock strength. When the thermal properties are linked with the porosity of the rock, an inverse relationship between the conductivity and diffusivity (i.e., a direct relationship to the specific heat) was observed with the previous properties.
6. Indirectly, the thermal properties of the lime building stone can be predicted through a set of mathematical models that relate the thermal properties with the physical and engineering properties. These mathematical models were developed by using regression analysis.
7. According to multivariate regression analysis, a strong correlation between thermal properties and rock's compressive strength was observed, where the UCS was termed in all multivariate regression models; therefore, it can be considered the most important factor affecting the thermal properties of the rock.
8. ANN models provide more accurate and better results in terms of R^2, RMSE, and applicability on a holdout sample (validation data set), especially for specific heat prediction as opposed to multivariate regression.

Author Contributions: Conceptualization, A.A.S., S.R.R. and M.O.T.; methodology, A.A.S., S.R.R. and M.O.T.; software, M.O.T. and H.A.A.; validation, H.A.; formal analysis, M.O.T. and H.A.A.; investigation, A.A.S., S.R.R. and M.O.T.; resources, A.A.S., S.R.R. and M.O.T.; data curation, S.R.R.; writing—original draft preparation, S.R.R. and M.O.T.; writing—review and editing, S.R.R., M.O.T. and H.A.; visualization, A.A.S., S.R.R. and M.O.T.; supervision, A.A.S. and S.R.R. All authors have read and agreed to the published version of the manuscript.

Funding: This research did not receive any specific grant from funding agencies.

Institutional Review Board Statement: Not applicable.

Informed Consent Statement: Not applicable.

Data Availability Statement: All data of this research were presented in the article.

Conflicts of Interest: The authors declare no conflict of interest.

References

1. Yaşar, E.; Erdoğan, Y. Strength and Thermal Conductivity in Lightweight Building Materials. *Bull. Eng. Geol. Environ.* **2008**, *67*, 513–519. [CrossRef]
2. Gul, I.H.; Maqsood, A. Thermophysical Properties of Diorites along with the Prediction of Thermal Conductivity from Porosity and Density Data. *Int. J. Thermophys.* **2006**, *27*, 614–626. [CrossRef]
3. Çengel, Y.A. *Heat Transfer: A Practical Approach*, 2nd ed.; McGraw-Hill: Boston, MA, USA, 2003.
4. Shi, X. Controlling Thermal Properties of Asphalt Concrete and Its Multifunctional Applications. Master's Thesis, Texas A&M University, College Station, TX, USA, 2014.
5. Labus, M.; Labus, K. Thermal Conductivity and Diffusivity of Fine-Grained Sedimentary Rocks. *J. Therm. Anal. Calorim.* **2018**, *132*, 1669–1676. [CrossRef]
6. Robertson, E.C. *Thermal Properties of Rocks*; US Department of the Interior: Washington, DC, USA; Geological Survey: Reston, VA, USA, 1988.
7. Sun, Q.; Lü, C.; Cao, L.; Li, W.; Geng, J.; Zhang, W. Thermal Properties of Sandstone after Treatment at High Temperature. *Int. J. Rock Mech. Min. Sci.* **2016**, *85*, 60–66. [CrossRef]
8. Stylianou, I.I.; Tassou, S.; Christodoulides, P.; Panayides, I.; Florides, G. Measurement and Analysis of Thermal Properties of Rocks for the Compilation of Geothermal Maps of Cyprus. *Renew. Energy* **2016**, *88*, 418–429. [CrossRef]
9. Çanakci, H.; Demirboğa, R.; Karakoç, M.B.; Şirin, O. Thermal Conductivity of Limestone from Gaziantep (Turkey). *Build. Environ.* **2007**, *42*, 1777–1782. [CrossRef]
10. Khandelwal, M. Prediction of Thermal Conductivity of Rocks by Soft Computing. *Int. J. Earth Sci.* **2010**, *100*, 1383–1389. [CrossRef]
11. Jones, M.Q.W. Thermal Properties of Stratified Rocks from Witwatersrand Gold Mining Areas. *J. South. African Inst. Min. Metall.* **2003**, *103*, 173–185.
12. Harmathy, T.Z. Thermal Properties of Concrete at Elevated Temperatures. *J. Mater.* **1970**, *5*, 47–74.
13. Ahadi, M.; Andisheh-Tadbir, M.; Tam, M.; Bahrami, M. An Improved Transient Plane Source Method for Measuring Thermal Conductivity of Thin Films: Deconvoluting Thermal Contact Resistance. *Int. J. Heat Mass Transf.* **2016**, *96*, 371–380. [CrossRef]
14. Troschke, B.; Burkhardt, H. Thermal Conductivity Models Fro Two-Phase Systems. *Phys. Chem. Earth* **1998**, *23*, 351–355. [CrossRef]
15. Clauser, C.; Huenges, E. Thermal Conductivity of Rocks and Minerals. In *Rock Physics and Phase Relations: A Handbook of Physical Constants*; John Wiley & Sons: Hoboken, NJ, USA, 2013; Volume 3, pp. 105–126.
16. Boulanouar, A.; Rahmouni, A.; Boukalouch, M.; Samaouali, A.; Géraud, Y.; Harnafi, M.; Sebbani, J. Determination of Thermal Conductivity and Porosity of Building Stone from Ultrasonic Velocity Measurements. *Geomaterials* **2013**, *3*, 138–144. [CrossRef]
17. Özkahraman, H.T.; Selver, R.; Işk, E.C. Determination of the Thermal Conductivity of Rock from P-Wave Velocity. *Int. J. Rock Mech. Min. Sci.* **2004**, *41*, 703–708. [CrossRef]
18. Han, H.; Yin, S. In-Situ Stress Inversion in Liard Basin, Canada, from Caliper Logs. *Petroleum* **2018**, *6*, 392–403. [CrossRef]
19. Maji, V.B.; Sitharam, T.G. Prediction of Elastic Modulus of Jointed Rock Mass Using Artificial Neural Networks. *Geotech. Geol. Eng.* **2008**, *26*, 443–452. [CrossRef]
20. Bui, D.K.; Nguyen, T.N.; Ngo, T.D.; Nguyen-Xuan, H. An Artificial Neural Network (ANN) Expert System Enhanced with the Electromagnetism-Based Firefly Algorithm (EFA) for Predicting the Energy Consumption in Buildings. *Energy* **2020**, *190*, 116370. [CrossRef]
21. Singh, T.N.; Sinha, S.; Singh, V.K. Prediction of Thermal Conductivity of Rock through Physico-Mechanical Properties. *Build. Environ.* **2007**, *42*, 146–155. [CrossRef]
22. Dweirj, M.; Fraige, F.; Alnawafleh, H.; Titi, A.; Dweirj, M.; Fraige, F.; Alnawafleh, H.; Titi, A. Geotechnical Characterization of Jordanian Limestone. *Geomaterials* **2017**, *7*, 1–12. [CrossRef]
23. NRAUT. *Geological and Engineering Study of Limestone Suitable for Construction Purposes in the Eastern Part of the Hashemite Kingdom of Jordan*; Natural Resources Authority Report; NRAUT: Amman, Jordan, 2003.
24. *ASTM D4543*; Practices for Preparing Rock Core as Cylindrical Test Specimens and Verifying Conformance to Dimensional and Shape Tolerances. ASTM International: West Conshohocken, PA, USA, 2019. [CrossRef]
25. He, Y. Rapid Thermal Conductivity Measurement with a Hot Disk Sensor: Part 1. Theoretical Considerations. *Thermochim. Acta* **2005**, *436*, 122–129. [CrossRef]
26. Chen, T.-G.; Yu, P.; Chou, R.-H.; Pan, C.-L. Phonon Thermal Conductivity Suppression of Bulk Silicon Nanowire Composites for Efficient Thermoelectric Conversion. *Opt. Express* **2010**, *18*, A467. [CrossRef]
27. Mirzanamadi, R.; Johansson, P.; Grammatikos, S.A. Thermal Properties of Asphalt Concrete: A Numerical and Experimental Study. *Constr. Build. Mater.* **2018**, *158*, 774–785. [CrossRef]
28. International Society for Rock Mechanics (ISRM). *The ISRM Suggested Methods for Rock Characterization, Testing and Monitoring: 2007–2014*; Ulusay, R., Ed.; Springer International Publishing: Cham, Switzerland, 2007; ISBN 978-3-319-07712-3.
29. *ASTM D2845*; Standard Test Method for Laboratory Determination of Pulse Velocities and Ultrasonic Elastic Constants of Rock. ASTM International: West Conshohocken, PA, USA, 2008.
30. *ASTM D5873*; Standard Test Method for Determination of Rock Hardness by Rebound Hammer Method. ASTM International: West Conshohocken, PA, USA, 2014.
31. *ASTM D7012*; Standard Test Method for Compressive Strength and Elastic Moduli of Intact Rock Core Specimens under Varying States of Stress and Temperatures. ASTM International: West Conshohocken, PA, USA, 2014.

32. *ASTM D5731*; Standard Test Method for Determination of the Point Load Strength Index of Rock and Application to Rock Strength Classifications. ASTM International: West Conshohocken, PA, USA, 2016. [CrossRef]
33. Islam, M.R.; Tarefder, R.A. Determining Thermal Properties of Asphalt Concrete Using Field Data and Laboratory Testing. *Constr. Build. Mater.* **2014**, *67*, 297–306. [CrossRef]
34. Cermak, V.; Rybach, L. Thermal Conductivity and Specific Heat of Minerals and Rocks. In *Geophysics—Physical Properties of Rocks*; Beblo, M., Ed.; Springer: Berlin/Heidelberg, Germany, 1982; pp. 305–343; ISBN 3540110704.
35. Pechnig, R.; Mottaghy, D.; Koch, A.; Jorand, R.; Clauser, C. Prediction of Thermal Properties for Mesozoic Rocks of Southern Germany. In Proceedings of the European Geothermal Congress, Unterhaching, Germany, 30 May–1 June 2007.
36. Rajabi, A.; Hosseini, A.; Heidari, A. The New Empirical Formula to Estimate the Uniaxial Compressive Strength of Limestone; North of Saveh a Case Study. *J. Eng. Geol.* **2017**, *11*, 159–180.
37. Mahdiyar, A.; Armaghani, D.J.; Marto, A.; Nilashi, M.; Ismail, S. Rock Tensile Strength Prediction Using Empirical and Soft Computing Approaches. *Bull. Eng. Geol. Environ.* **2019**, *78*, 4519–4531. [CrossRef]
38. Barham, W.S.; Rabab'ah, S.R.; Aldeeky, H.H.; Al Hattamleh, O.H. Mechanical and Physical Based Artificial Neural Network Models for the Prediction of the Unconfined Compressive Strength of Rock. *Geotech. Geol. Eng.* **2020**, *38*, 4779–4792. [CrossRef]
39. Pichugin, Z.; Chekhonin, E.; Popov, Y.; Kalinina, M.; Bayuk, I.; Popov, E.; Spasennykh, M.; Savelev, E.; Romushkevich, R.; Rudakovskaya, S. Weighted Geometric Mean Model for Determining Thermal Conductivity of Reservoir Rocks: Current Problems with Applicability and the Model Modification. *Geothermics* **2022**, *104*, 102456. [CrossRef]
40. Zeb, A.; Misbah; Maqsood, A. Prediction of Effective Thermal Conductivity of Consolidated Porous Materials under Ambient Conditions. *Indian J. Phys.* **2014**, *88*, 603–607. [CrossRef]
41. Chekhonin, E.; Popov, Y.; Romushkevich, R.; Popov, E.; Zagranovskaya, D.; Zhukov, V. Integration of Thermal Core Profiling and Scratch Testing for the Study of Unconventional Reservoirs. *Geosciences* **2021**, *11*, 260. [CrossRef]
42. Feng, X.; Jimenez, R. Bayesian Prediction of Elastic Modulus of Intact Rocks Using Their Uniaxial Compressive Strength. *Eng. Geol.* **2014**, *173*, 32–40. [CrossRef]
43. Pallant, J. *SPSS Survival Manual: A Step by Step Guide to Data Analysis Using IBM SPSS*; Routledge: London, UK, 2020; ISBN 1003117457.
44. Larson-Hall, J. *A Guide to Doing Statistics in Second Language Research Using SPSS and R*; Routledge: London, UK, 2015; ISBN 1315775662.
45. Hornik, K.; Stinchcombe, M.; White, H. Multilayer Feedforward Networks Are Universal Approximators. *Neural Netw.* **1989**, *2*, 359–366. [CrossRef]
46. Gardner, M.W.; Dorling, S.R. Artificial Neural Networks (the Multilayer Perceptron)—A Review of Applications in the Atmospheric Sciences. *Atmos. Environ.* **1998**, *32*, 2627–2636. [CrossRef]